Thermal decomposition of n-propyl and n-butyl nitrates: kinetics and products

JULIEN MORIN and YURI BEDJANIAN*

Institut de Combustion, Aérothermique, Réactivité et Environnement (ICARE), CNRS and Université d'Orléans, 45071 Orléans Cedex 2, France

ABSTRACT. Thermal decomposition of n-propyl ($C_3H_7ONO_2$, PPN) and n-butyl ($C_4H_9ONO_2$, BTN) nitrates have been studied in a low pressure flow reactor combined with a quadrupole mass spectrometer. The rate constants of the nitrates decomposition were measured as a function of pressure (0.95 -12.8 Torr of helium) and temperature in the range 473 – 659 K using two different approaches: from kinetics of nitrate loss and those of the formation of the reaction products. The fit of the observed falloff curves with two parameter expression $k = \frac{k_0 k_\infty [M]}{k_0[M] + k_\infty} \times 0.6^{(1+(\log(\frac{k_0[M]}{k_\infty}))^2)^{-1}}$ provided the following low and high pressure limits for the rate constants of the nitrates decomposition: k_0(PPN) = 0.68× 10^{-4} exp(-15002/T) $cm^3molecule^{-1}s^{-1}$, k_∞ (PPN) = 7.34× 10^{15} exp(-19676/T) s^{-1}, k_0(BTN) = 2.80× 10^{-4} exp(-15382/T) $cm^3molecule^{-1}s^{-1}$ and k_∞(BTN) = 7.49× 10^{15} exp(-19602/T) s^{-1}, which allow to reproduce (via above expression and with 20% uncertainty) all the experimental data obtained for the rate constants of PPN and BTN decomposition in the temperature and pressure range of the study. It was observed that the initial step of the thermal decomposition of the nitrates is O–NO_2 bond cleavage leading to formation of NO_2 and alkoxy radical, which rapidly decomposes or isomerizes to form C_2H_5 and formaldehyde and C_3H_7, CH_2O and hydroxybutyl radical as final products of PPN and BTN decomposition, respectively. In addition, the kinetic data were used to determine the O-NO_2 bond dissociation energy of 38.0 ± 1.2 and 37.8 ± 1.0 kcal mol^{-1} in PPN and BTN, respectively.

Keywords: propyl nitrate, butyl nitrate, thermal decomposition, rate constant, falloff curve, alkoxy radical.

*Corresponding author

E-mail address: yuri.bedjanian@cnrs-orleans.fr (Yuri Bedjanian)

1. Introduction

Organic nitrates are important species in atmospheric and combustion chemistry. In the atmosphere, they are formed in a minor addition channel of the reaction of peroxy radicals with NO and also in the NO_3-initiated oxidation of unsaturated organic compounds [1]. Organic nitrates are considered as stable species with atmospheric lifetimes of several days or weeks (depending on their photolysis rate and reactivity toward OH radicals [2]), and play a key role in the distribution of reactive nitrogen by undergoing long-range transport in the free troposphere. In combustion processes, nitrates, used as fuel additives, are known to promote the ignition of diesel fuel. Production of chain-initiating radicals and, possibly, the heat released during nitrate decomposition in the pre-ignition phase are thought to decrease the ignition-delay time [3-5].

Thermal decomposition of acyclic nitrates is supposed to proceed through a radical mechanism with initial dissociation of the O–NO_2 bond leading to formation of NO_2 and alkoxy radical (RO):

$$RONO_2 \rightarrow RO + NO_2$$

The alkoxy radicals can undergo a number of competing reaction pathways, including unimolecular decomposition, which usually occurs through C-C bond fission to produce a carbonyl compound, and a unimolecular isomerization, which generates a hydroxy-substituted alkyl radical [6].

Although thermal decomposition of nitrates has been studied previously for several times [7-15], available quantitative information on the rate constants and products of these reactions is very scarce. To our knowledge, no experimental data are available for thermal decomposition of n-butyl nitrate and those for n-propyl nitrate pyrolysis were reported in two studies only [13,16]. In our recent paper [17], we have reported the results of the experimental study of the kinetics and products of the thermal decomposition of isopropyl nitrate. In the

present work, we applied a similar experimental approach to study thermal decomposition of n-propyl (PPN) and n-butyl (BTN) nitrates, including the measurements of the rate constants as a function of pressure and temperature and identification and quantification of the reaction products:

$CH_3CH_2CH_2ONO_2$ (+M) → products (1)

$CH_3CH_2CH_3CH_2ONO_2$ (+M) → products (2)

2. Materials and methods

Thermal decomposition of the nitrates was studied at a total pressure of helium between 0.95 and 12.8 Torr and in the temperature range (473 - 659) K. Experiments were carried out in a flow reactor using a modulated molecular beam electron impact ionization (with ion source operating at 25-30 eV) mass spectrometer as the detection method [17,18]. The flow reactor (Fig. 1) consisted of a Quartz tube (45 cm length and 2.5 cm i.d.) with an electrical heater and water-cooled extremities [18]. Temperature in the reactor was measured with a *K*-type thermocouple positioned in the middle of the reactor in contact with its outer surface. Temperature gradient along the flow tube measured with a thermocouple inserted in the reactor through the movable injector was less than 1% [18].

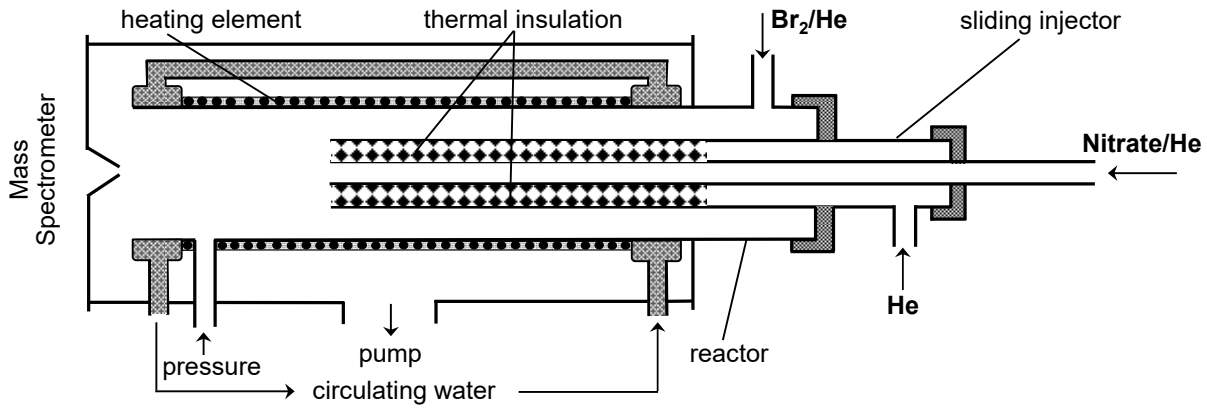

Fig. 1 Diagram of the flow reactor.

The nitrates were introduced into the flow reactor through the movable injector (that allowed to vary their residence time in the reactor) from a 10L flasks containing nitrate-He mixture or (when high concentrations of the nitrates were needed) by passing helium through a thermostated glass bubbler containing liquid nitrate. The inner tube of the injector, through which nitrates were supplied, was thermally insulated in order to minimize their possible decomposition prior introduction into the main reactor (Fig. 1). Both nitrates was detected by mass spectrometry at their fragment peak at *m/z* = 76 ($CH_2ONO_2^+$), which is much more intensive than the parent ones (at *m/z* = 105 and 119, for PPN and BTN, respectively). C_2H_5, C_3H_7 and hydroxybutyl ($C^{\bullet}H_2CH_2CH_2CH_2OH$) radicals were detected as bromoethane, 1-bromopropane and 4-bromo-1-butanol at m/z = 108/110 ($C_2H_5Br^+$), 122/124 ($C_3H_7Br^+$) and fragment peak 134/136 ($CH_2Br(CH_2)_2CH^+$), respectively, after being scavenged by an excess of Br_2 ([Br_2] ~5×10^{13} molecule cm^{-3}) via reactions [19]:

$$C_2H_5 + Br_2 \rightarrow C_2H_5Br + Br \quad (3)$$

$$C_3H_7 + Br_2 \rightarrow C_3H_7Br + Br \quad (4)$$

$$CH_2(CH_2)_3OH + Br_2 \rightarrow CH_2Br(CH_2)_3OH + Br \quad (5)$$

All other species were detected at their parent peaks: *m/z*= 30 (formaldehyde, CH_2O^+), 160 (Br_2^+), 46 (NO_2^+).

The absolute calibration of mass spectrometer for formaldehyde was realized by injecting known amounts (0.2−0.8 μL) of the 36.5 % wt solution of CH_2O in water inside the flow tube, and recording the parent mass peak intensity of CH_2O at m/z = 30. The integrated area of the mass spectrometric signals corresponding to known total number of CH_2O molecules injected into the reactor allowed the determination of the calibration factor. Similar procedure was applied for the measurements of the absolute concentrations of 4-bromo-1-butanol. Another alternative method used for absolute calibrations of CH_2O consisted in thermal decomposition of ethyl nitrate (at T ≥ 600K) in the presence of Br_2 in the reactor:

$CH_3CH_2ONO_2$ (+M) → $CH_3 + CH_2O + NO_2$ (+M) (6)

(products of this reaction were studied in an unpublished work from our group). Experimentally, total consumption of the nitrate and appearance of the decomposition products, NO_2 and CH_2O, was observed and absolute concentrations of the species could be determined in accordance with: $[CH_2O] = [NO_2] = [C_2H_5ONO_2]_0$. The results of this calibration method were in good agreement (within 10-15%) with that by injection of CH_2O and measurements of $[NO_2]$ from their calibrated mixtures. The absolute calibration of mass spectrometer for other stable species (Br_2, C_2H_5Br, C_3H_7Br, $C_2H_5ONO_2$, $C_3H_7ONO_2$, $C_4H_7ONO_2$) was realized through calculation of their absolute concentrations in the reactor from their flow rates obtained from the measurements of the pressure drop of their mixtures in He stored in calibrated volume flasks.

Ethyl and n-propyl nitrates were synthesized in the laboratory via slow mixing of the corresponding alcohol with H_2SO_4:HNO_3 (1:1) mixture at temperature < 5°C [20,21]. The synthesized nitrate was degassed before use. The purities and origin of other gases used were as follows: He >99.9995% (Alphagaz); Br_2 >99.99% (Aldrich); NO_2 > 99% (Alphagaz); 36.5 % wt solution of formaldehyde in water (Sigma-Aldrich); n-butyl nitrate > 99% (Chemos); bromoethane (≥ 99%, Sigma-Aldrich); 1-bromopropane (≥ 99%, Sigma-Aldrich); 4-bromo-1-butanol (≥ 85%, Aldrich).

3. Results and discussion

We employed two different methods for the measurements of the rate of nitrate decomposition [17]. The first one, used at higher temperatures (T = 563 – 659 K), consisted in a direct monitoring of the kinetics of nitrate loss. In the second approach, used at lower temperatures (T = 473 – 577 K), where consumption of nitrate was too low to be measured

accurately, the rate constant was determined from the kinetics of the reaction product formation.

3.1. Kinetics of n-propyl and n-butyl nitrate decomposition

In this series of experiments the rate constant of reactions (1) and (2) was determined from the kinetics of nitrate loss due to its decomposition. It was observed that at a given total pressure consumption of nitrate follows first order kinetics: d[Nitrate]/dt = -k×[Nitrate]. Example of the exponential decays of n-propyl nitrate observed at different pressures in the reactor at T = 627 K is shown in Fig. 2.

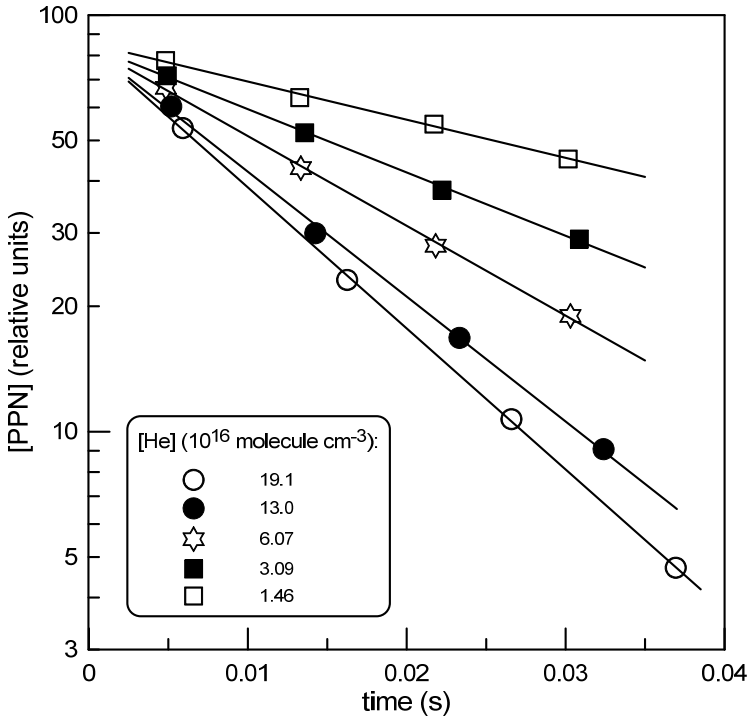

Fig. 2 Example of kinetics of n-propyl nitrate decomposition at different pressures of He in the reactor: T = 627 K.

The values of k_1 and k_2 (in s^{-1}) determined from the loss kinetics of PPN and BTN (like those shown in Fig. 2) at different temperatures in the reactor are plotted in Fig. 3 and 4 as a function of total pressure. The uncertainty on the measurements of the rate constants was estimated to be nearly 10%, including statistical error (within a few percent) and those on the measurements of the flows (5%), pressure (2%) and temperature (1%).

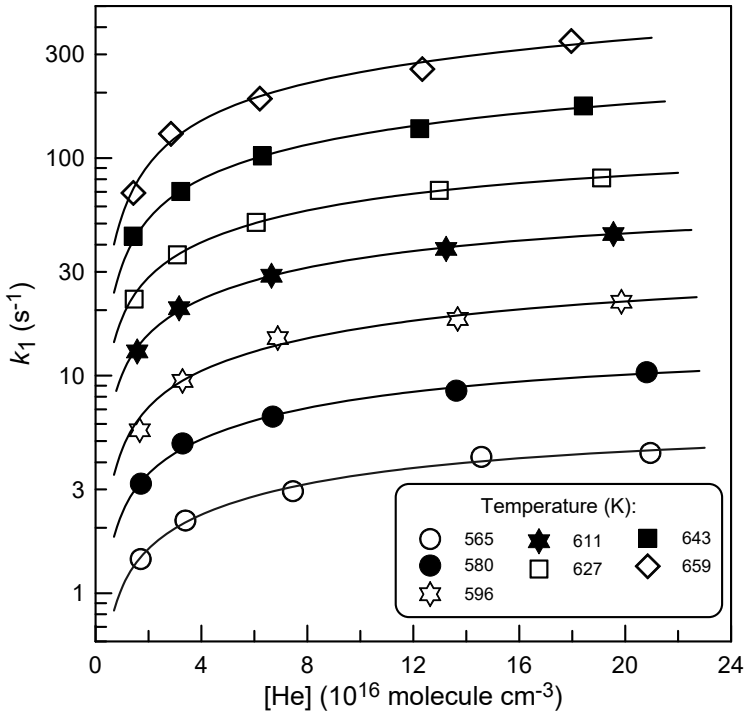

Fig. 3 Rate of n-propyl nitrate decomposition measured at different temperatures from kinetics of the nitrate loss as a function of total pressure of He. Uncertainty on k_1 (nearly 10%) corresponds to the size of symbols. Continuous lines represent the best fit to the experimental data according to equations (I) and (II) with $F_c = 0.6$ and two varied parameters, k_0 and k_∞.

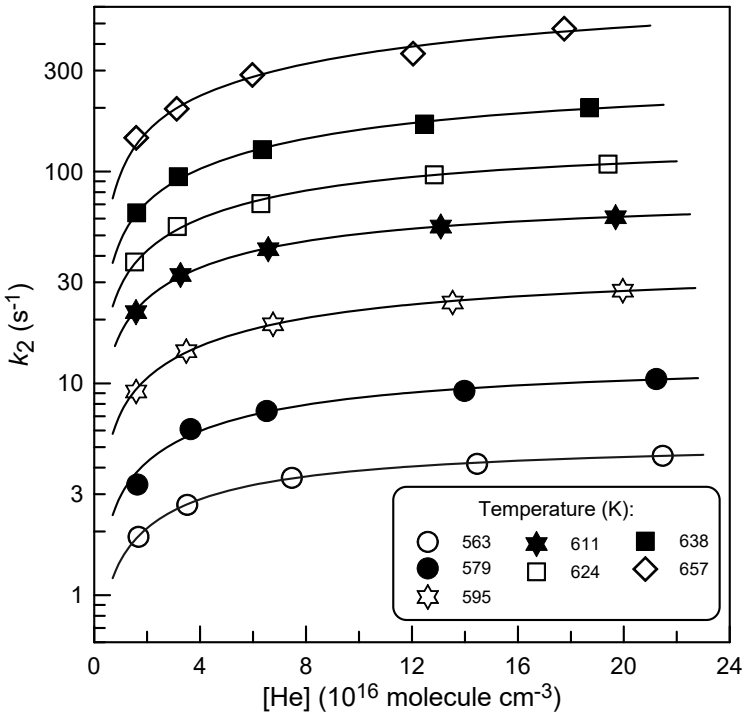

Fig. 4 Rate of n-butyl nitrate decomposition measured at different temperatures from kinetics of BTN loss as a function of total pressure of He. Uncertainty on k_2 (nearly 10%) corresponds to the size of symbols. Continuous lines represent the best fit to the experimental data according to equations (I) and (II) with $F_c = 0.6$ and two varied parameters, k_0 and k_∞.

One can note that in the pressure range of the present study, decomposition of nitrates proceeds in the "falloff regime" (Fig. 3 and 4). Generally the dependence of the rate constant on pressure in falloff regime is described using the Lindemann-Hinshelwood reaction scheme:

$$AB + M \leftrightarrows AB^* + M \quad (7,\text{-}7)$$

$$AB^* \rightarrow A + B \quad (8)$$

with addition of a broadening factor, F, to the Lindemann-Hinshelwood expressions [22,23], leading to

$$k = \frac{k_0 k_\infty [\mathrm{M}]}{k_0[\mathrm{M}] + k_\infty} F = k_0[\mathrm{M}] \left(\frac{1}{1 + k_0[\mathrm{M}]/k_\infty} \right) F \quad (\mathrm{I})$$

where $k_0 = k_7$ and $k_\infty = k_7 k_8 / k_{-7}$ are low and high pressure limits of the rate constant, respectively, and the broadening factor F is determined as:

$$\log F \cong \frac{\log F_c}{1 + \left(\frac{\log(k_0[\mathrm{M}]/k_\infty)}{N} \right)^2} \quad (\mathrm{II})$$

with $N = 0.75\text{-}1.27 \log F_c$ [22,23]. So the falloff curve is characterized by three parameters, k_0, k_∞ and F_c (called "center broadening factor"), all being reaction- and temperature-dependent. In practice, it is impossible to fit a limited part of falloff curve, usually determined in experiments, with three variable parameters. In the present study, as in our previous work on decomposition of isopropyl nitrate [17], in order to describe the dependence of the rate constant on pressure we adopted simplified approach used in JPL evaluation of kinetic data [24]: the experimental falloff curve was fitted accordingly to equations (I) and (II) with fixed and independent of temperature $F_c = 0.6$ and $N = 1$ and two varied parameters, k_0 and k_∞. Obviously, k_0 and k_∞ determined in this way depend on the choice of F_c-value, nevertheless this procedure allows to describe the experimental data with the three clearly specified parameters.

Continuous lines in Fig. 3 and 4 represent the fit to the experimental data according to equations (I) and (II) with F_c = 0.6, providing the values of k_0 and k_∞ for decomposition of PPN and BTN at different temperatures, which are summarized in Tables I and II, respectively.

Table I

Thermal decomposition of n-propyl nitrate: summary of the measurements of k_0 and k_∞.

T (K)	k_0 (10^{-15} cm^{3}molecule^{-1}s^{-1}) [a]	k_∞ (s^{-1}) [a]	Method [b]
473	0.00101	0.00635	C_2H_5 kinetics
488	0.00237	0.0264	C_2H_5 kinetics
503	0.00811	0.0753	C_2H_5 kinetics
518	0.0163	0.231	C_2H_5 kinetics
533	0.0492	0.647	C_2H_5 kinetics
549	0.105	1.66	C_2H_5 kinetics
564	0.198	4.66	C_2H_5 kinetics
565	0.196	7.45	PPN kinetics
577	0.360	8.83	C_2H_5 kinetics
580	0.419	17.2	PPN kinetics
596	0.747	41.5	PPN kinetics
611	1.77	78.8	PPN kinetics
627	3.19	147	PPN kinetics
643	4.74	389	PPN kinetics
659	8.08	853	PPN kinetics

[a] estimated uncertainty factor of 1.5,
[b] see text.

Table II

Thermal decomposition of n-butyl nitrate: summary of the measurements of k_0 and k_∞.

T (K)	k_0 (10^{-15} cm^{3}molecule^{-1}s^{-1}) [a]	k_∞ (s^{-1}) [a]	Method [b]
484	0.00470	0.019	products kinetics
499	0.0120	0.071	products kinetics
514	0.0259	0.205	products kinetics
531	0.090	0.612	products kinetics
545	0.183	1.65	products kinetics
561	0.411	4.8	products kinetics

563	0.394	6.06	BTN kinetics
579	0.676	15	BTN kinetics
595	1.51	41.7	BTN kinetics
611	3.92	89.6	BTN kinetics
624	6.00	167	BTN kinetics
638	8.65	341	BTN kinetics
657	15.7	926	BTN kinetics

[a] estimated uncertainty factor of 1.5,
[b] see text.

The measurements of k_1 and k_2 were carried out with initial concentration of nitrate $\leq 10^{12}$ molecule cm^{-3}. In a special series of experiments, we have verified for the possible influence of the initial concentration of PPN (at P = 8.3 Torr and T = 602 K) and BTN (at P = 8.2 Torr and T = 611 K) on the measured values of k_1 and k_2. The rates of PPN and BNT decomposition were found to be independent (within 5%, for PPN see Fig. S1 in Supplementary data) of their initial concentrations varied in the range (0.09 – 2.40) and (0.15 – 1.90)$\times 10^{12}$ molecule cm^{-3}, respectively.

Decomposition of the nitrates on the wall of the flow reactor could potentially impact the measured rates of their loss. Adams & Bawn [8] in their study of ethyl nitrate decomposition under static conditions reported that a 7.4 times increase in surface of a Pyrex reaction vessel had no influence on the reaction rate at T = 456 K, indicating on a limited impact of the wall processes. This finding allows to expect a negligible (compared with homogeneous process) heterogeneous loss of PPN and BTN in our fast flow quartz reactor, although in the present study the decomposition of the nitrates on the wall of the reactor was not tested.

3.2. Reaction products

Thermal decomposition of n-propyl nitrate is expected to proceed through initial dissociation of the O–NO_2 bond leading to formation of NO_2 and propoxy radical:

$$CH_3CH_2CH_2ONO_2\ (+M) \rightarrow CH_3CH_2CH_2O + NO_2\ (+M) \qquad (1)$$

The n-propoxy radical, $CH_3CH_2CH_2O$, can undergo unimolecular decomposition through the following two competitive reaction pathways [6,25]:

$$CH_3CH_2CH_2O\ (+M) \rightarrow C_2H_5 + CH_2O\ (+M) \quad (9a)$$

$$CH_3CH_2CH_2O\ (+M) \rightarrow H + CH_3CH_2CHO\ (+M) \quad (9b)$$

Based on the rate constants calculated for reactions (9a) and (9b) [6,25], one could expect that under experimental conditions of the present study (i) C_2H_5 forming channel (9a) is the dominant one ($k_{9b}/k_{9a} < 0.002$) and (ii) decomposition of the n-propoxy radical is very rapid on the timescale of our experiments ($k_{9a} > 10^4$ s^{-1}). Indeed, we have observed the formation of NO_2, C_2H_5 and formaldehyde (CH_2O) upon decomposition of n-propyl nitrate in the flow reactor. There is an important contribution of n-propyl nitrate to the MS signals of NO_2 and CH_2O due to its fragmentation in the ion source of the mass spectrometer. That is why the quantitative measurements of the yields of the three reaction products were carried out under conditions where almost complete decomposition of PPN was observed. Experiments consisted in the monitoring of the concentrations of the products formed upon total decomposition of PPN in the reactor in the presence of relatively high concentration of Br_2 ($[Br_2]$ ~5×10^{13} molecule cm^{-3}) in order to transform C_2H_5 radicals into C_2H_5Br. Initial concentration of PPN was varied in the range $(0.13 – 1.61)\times10^{12}$ molecule cm^{-3}. The results of these experiments are shown in Fig. 5.

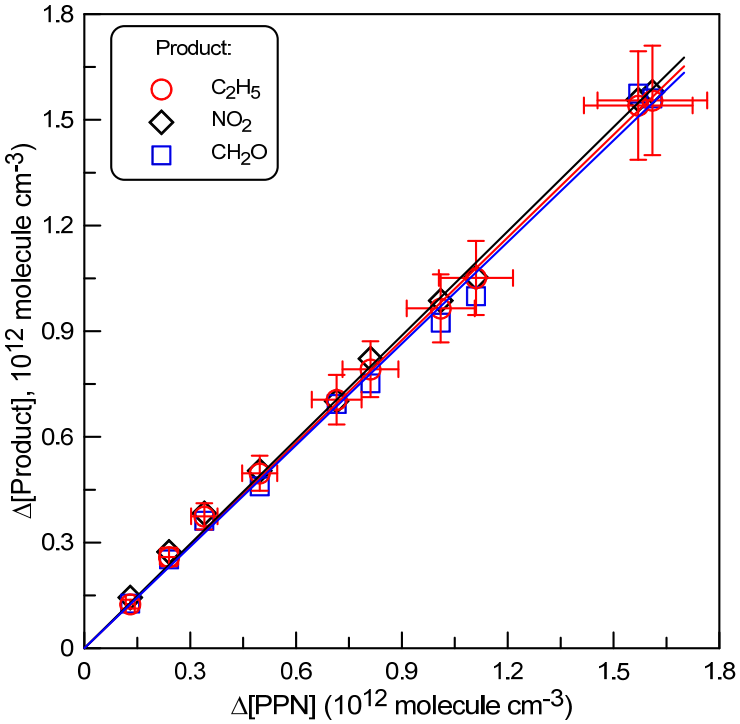

Fig. 5 Concentration of the products formed upon decomposition of n-propyl nitrate as a function of consumed concentration of PPN: P = 8.5 Torr, T = 630 K. Error bars correspond to 10% uncertainty on the measurements of the PPN and product concentrations.

The slopes of the straight lines in Fig. 5 provide the yields of the corresponding species:

$\Delta[NO_2]/\Delta[PPN] = 0.99 \pm 0.15$,

$\Delta[CH_2O]/\Delta[PPN] = 0.96 \pm 0.15$,

$\Delta[C_2H_5]/\Delta[PPN] = 0.97 \pm 0.15$,

The estimated nearly 15% uncertainty on the measurements arises mainly from the combined errors on the measurements of the absolute concentrations of n-propyl nitrate and reaction products. These results confirm that the O–NO_2 bond cleavage is the initial step of PPN decomposition and C-C bond fission leading to formation of C_2H_5 and formaldehyde is the predominant decomposition pathway of the n-propoxy radical under experimental conditions of the study.

In the case of reaction (2), the situation is somewhat more complex. The 1-butoxy radical ($CH_3CH_2CH_2CH_2O^\bullet$) formed upon decomposition of n-butyl nitrate,

$$CH_3CH_2CH_2CH_2ONO_2\ (+M) \rightarrow CH_3CH_2CH_2CH_2O^\bullet + NO_2\ (+M) \qquad (2)$$

in addition to its decomposition, can also isomerize to four hydroxybutyl radicals: $CH_3CH_2CH_2C^{\bullet}HOH$, $CH_3CH_2C^{\bullet}HCH_2OH$, $CH_3C^{\bullet}HCH_2CH_2OH$ and $C^{\bullet}H_2CH_2CH_2CH_2OH$. The available experimental and theoretical data [26] show that under the experimental conditions of the present study (temperature and pressure range) the dominant processes of 1-butoxy radical transformation are its decomposition to propyl radical and formaldehyde and isomerization to $C^{\bullet}H_2CH_2CH_2CH_2OH$ hydroxybutyl radical:

$$CH_3CH_2CH_2CH_2O^{\bullet} (+M) \rightarrow CH_3CH_2CH_2 + CH_2O (+M) \quad (10)$$

$$CH_3CH_2CH_2CH_2O^{\bullet} (+M) \leftrightarrow C^{\bullet}H_2CH_2CH_2CH_2OH (+M) \quad (11,-11)$$

The most favorable channels for the $C^{\bullet}H_2CH_2CH_2CH_2OH$ radical are its back isomerization to 1-butoxy radical (reaction (–11)) and decomposition to C_3H_7 and CH_2O [26]:

$$C^{\bullet}H_2CH_2CH_2CH_2OH (+M) \rightarrow CH_3CH_2CH_2 + CH_2O (+M) \quad (12)$$

In the presence of bromine in our flow reactor, the propyl and hydroxybutyl radicals are expected [19] to react with Br_2 to form 1-bromopropane and 4-bromo-1-butanol, respectively:

$$CH_3CH_2CH_2+Br_2 \rightarrow CH_3CH_2CH_2Br + Br \quad (4)$$

$$C^{\bullet}H_2CH_2CH_2CH_2OH + Br_2 \rightarrow CH_2BrCH_2CH_2CH_2OH + Br \quad (5)$$

Indeed, in our experiments on thermal decomposition of n-butyl nitrate in the presence of Br_2 we have observed the production of both 1-bromopropane ($C_3H_7Br^+$ at m/z = 122/124) and 4-bromo-1-butanol (at its fragment peaks at m/z = 134/136). It was observed that the distribution of these two brominated reaction products depended on the concentration of Br_2 in the reactor: increase of Br_2 concentration resulted in increase of 4-bromo-1-butanol and decrease of 1-bromopropane yield. This experimental observation reflects the concurrent consumption of $C^{\bullet}H_2CH_2CH_2CH_2OH$ radical in reactions (-11), (12) and (5). In addition, relative concentrations of 1-bromopropane and 4-bromo-1-butanol were found to depend also

on pressure and temperature because reactions (10) – (12) have different pressure and temperature dependences.

The results of the measurements of the yields of the products formed upon decomposition of BTN in the presence of Br_2 (~5×10^{13} molecule cm^{-3}) in the reactor at T = 640 K are shown in Fig. 6.

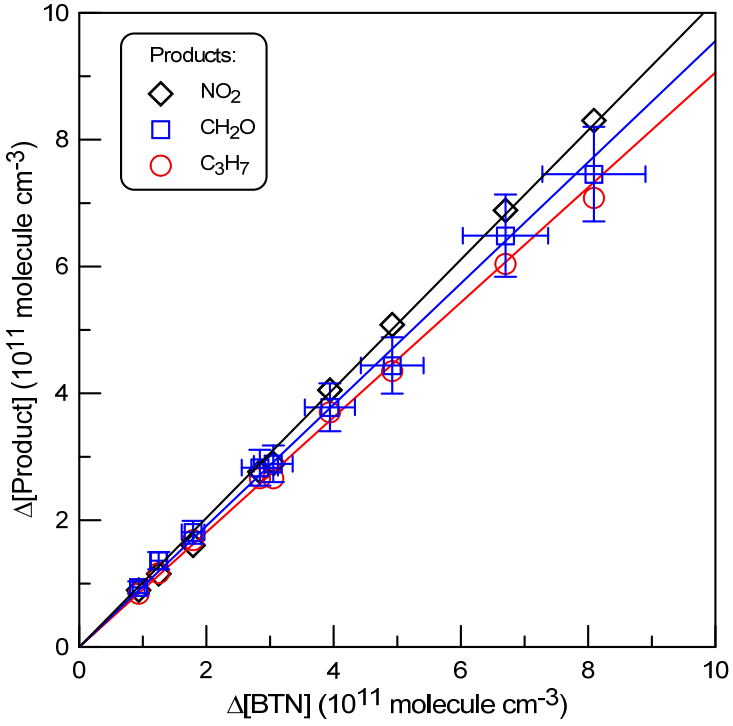

Fig. 6 Concentration of the products formed upon decomposition of n-butyl nitrate as a function of consumed concentration of BTN: P = 4 Torr, T = 640 K. Error bars correspond to characteristic 10% uncertainty on the measurements of the concentrations of BTN and reaction products.

The slopes of the straight lines in Fig. 6 provide the yields of the corresponding species:

$\Delta[NO_2]/\Delta[PPN] = 1.02 \pm 0.15$,

$\Delta[CH_2O]/\Delta[PPN] = 0.96 \pm 0.15$,

$\Delta[C_3H_7]/\Delta[PPN] = 0.91 \pm 0.15$,

The yield of 4-bromo-1-butanol, which was found to have a trend to decrease with increase of temperature, was measured to be < 5% in these experiments.

As noted above, the products of the thermal decomposition of propyl and butyl nitrates were investigated in the presence of Br_2 in the reactor leading to formation of Br atoms in reactions (3-5). The concentration of Br atoms in the reactor is expected to be similar to those of the reaction products, i.e. $\leq 1.6\times10^{12}$ molecule cm^{-3}. The possible side reactions of Br atoms with brominated alkanes C_2H_5Br and C_3H_7Br are relatively slow and have a negligible impact on the concentrations of these species under experimental conditions of the measurements. The rate constant of the reaction of Br with C_3H_7Br was reported in only one study:

$$Br + C_3H_7Br + M \rightarrow CH_3CHCH_2Br + HBr \quad (13)$$

$k_{13} = 2.09\times10^{-12}\exp(-3580/T)$ $cm^3molecule^{-1}s^{-1}$ (T = 374-483K) [27],

providing $k_{13} \approx 7.8\times10^{-15}$ $cm^3molecule^{-1}s^{-1}$ at highest temperature of the measurements T = 640K, i.e. $k'_{13} = k_{13}\times$ [Br] < 0.01 s^{-1}. The reaction of Br atoms with C_2H_5Br is expected to be even slower. Another reaction which potentially could have an impact on the observed products of reactions (1) and (2) is the reaction of Br atoms with CH_2O:

$$Br + CH_2O \rightarrow HBr + CHO \quad (14)$$

$k_{14} = 7.7\times10^{-12}\exp(-580/T)$ $cm^3molecule^{-1}s^{-1}$ (T = 220-300K) [28].

No data for the reaction rate constant are available at high temperatures. Extrapolation of the existing measurements to T = 630 K gives the value of the rate constant of nearly 3×10^{-12} $cm^3molecule^{-1}s^{-1}$. Even with maximal concentration of [Br] = 1.6×10^{12} molecule cm^{-3} the consumption of CH_2O in reaction with Br at T = 630 K would be less than 15% (reaction time ≈ 30 ms). The observed linear dependence of the concentrations of the reaction products on the consumed concentration of the nitrate (Fig. 5 and 6) can be considered as an additional experimental evidence of the negligible role of the secondary reactions of Br atoms.

3.3. Measurements of k_1 and k_2 from kinetics of product formation

In this series of experiments, carried out at lower temperatures, the rate constants of reactions (1) and (2) were determined from the kinetics of product formation under conditions where consumption of the nitrates was negligible and the rate constants could not be determined from their decays. For reaction (1), CH_3CH_2 radical was chosen among three products of PPN decomposition because the mass spectra of NO_2 and formaldehyde were highly perturbed by contribution of the fragment peaks of n-propyl nitrate which was present in the reactor at relatively high concentrations. Br_2 was added in the reactor in order to convert C_2H_5 radicals to C_2H_5Br, which was monitored by mass spectrometry. As one could expect, linear increase of C_2H_5 concentration with reaction time was observed upon decomposition of n-propyl nitrate (Fig. S2 in Supplementary data) in line with expression:

$$d[C_2H_5]/dt = k_1 \times [PPN] \qquad \text{(III)}$$

and under conditions where variation of PPN concentration with time was insignificant (< 10%). The slopes of the straight lines in Fig. S2 provide the rate of C_2H_5 production, $d[C_2H_5]/dt$ (in molecule $cm^{-3}s^{-1}$), which is presented in Fig. S3 (Supplementary data) as a function of initial concentration of PPN. The observed linear, in accordance with equation (III), dependence of $d[C_2H_5]/dt$ on [PPN] indicates negligible contribution of possible secondary reactions which could lead to C_2H_5 production or consumption.

Example of kinetics of C_2H_5 formation measured at different pressures in the reactor is shown in Fig. 7. All the experimental data obtained for k_1 ($k_1 = 1/[PPN] \times d[C_2H_5]/dt$) from the kinetics of C_2H_5 production at different pressures and temperatures are shown in Fig. 8. Procedure, similar to that used above in the case of PPN loss kinetics, was employed to extract low and high pressure limits of k_1: continuous lines in Fig. 8 represent the best fit to the experimental data according to equations (I) and (II) with $F_c = 0.6$ and two varied

parameters, k_0 and k_∞. The results obtained for k_0 and k_∞ in this series of experiments are presented in Table I.

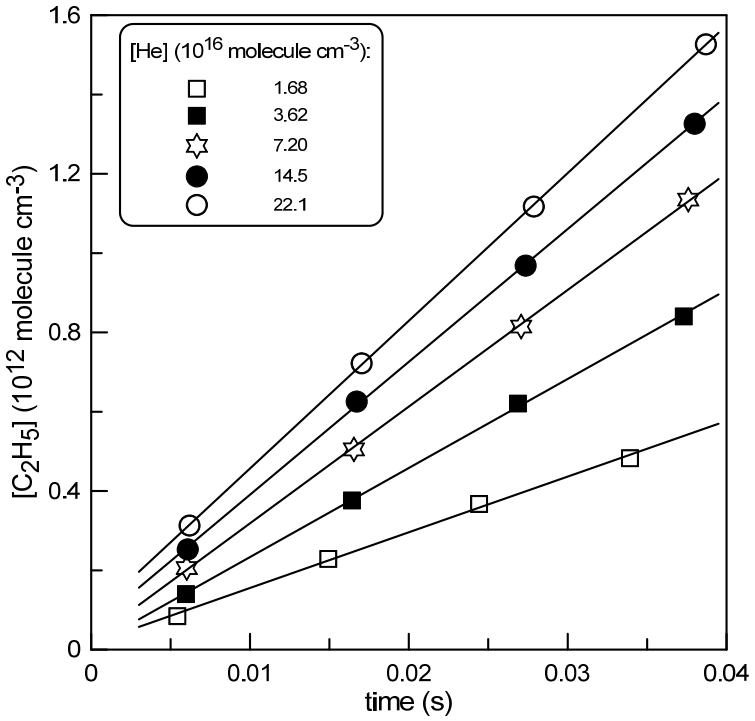

Fig. 7 Kinetics of C_2H_5 production upon PPN decomposition measured at different pressures in the reactor: T = 549 K, [PPN] = 3.0×10^{13} molecule cm^{-3}.

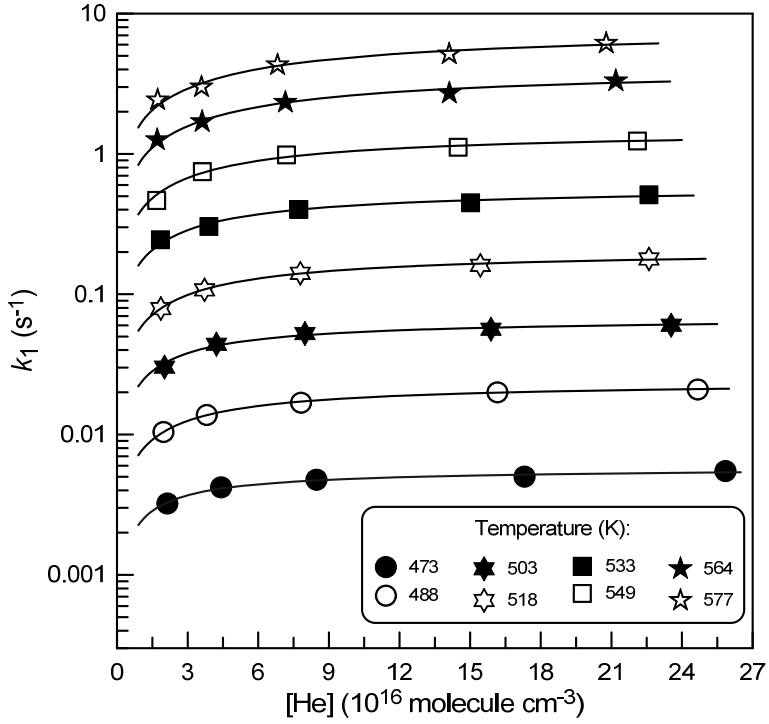

Fig. 8 Rate constant of C_2H_5 production upon PPN decomposition as a function of total pressure of He at different temperatures in the reactor. Height of the symbols corresponds to nearly 15% uncertainty on k_1.

Similar approach was employed for the measurements of k_2. However, in this case, given the complex dependence of the yields of the two main brominated products, 1-bromopropane and 4-bromo-1-butanol, on pressure, temperature and concentration of Br_2, in the measurements of k_2 from the kinetics of product formation we used the sum of the concentrations of these species, disregarding the distribution between them. The experimental data obtained for k_2 ($k_2 = 1/[BTN]\times d([C_3H_7]+[C^{\bullet}H_2(CH_2)_3OH])/dt$) at different pressures and temperatures are shown in Fig. 9.

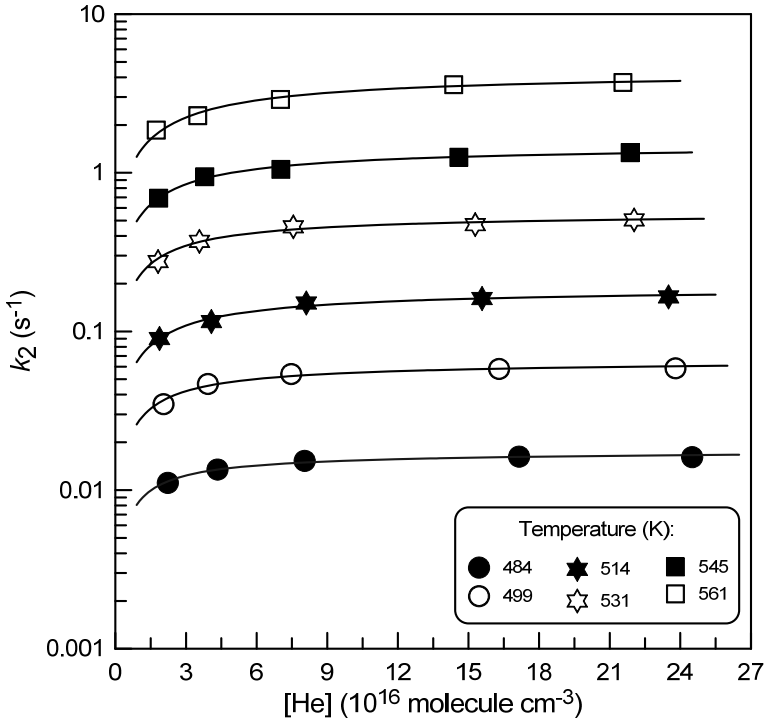

Fig. 9 Rate constant of reaction (2) measured from the kinetics of 1-bromopropane and 4-bromo-1-butanol production upon BTN decomposition in the presence of Br_2 as a function of total pressure of He at different temperatures in the reactor. Height of the symbols corresponds to nearly 15% uncertainty on k_2.

Low and high pressure limits of k_2, resulting from the best fit to the experimental data in Fig. 9 according to equations (I) and (II) with $F_c = 0.6$, are presented in Table 2.

Concerning the uncertainty on k_0 and k_∞ derived from the fit of the falloff curves (with fixed value of $F_c = 0.6$) in Fig. 3, 4, 8 and 9, it depends on the temperature of the

measurements and has a different trend for low and high pressure limits of k_1 and k_2. For example, it is obvious that at lower temperatures (Fig. 8 and 9), the simulated falloff curve is more sensible to the value of k_∞ and less to the value of k_0, because k_1 and k_2 are relatively close to their high pressure limits. To keep things simple, we place a conservative (nearly maximum) estimated uncertainty of a factor of 1.5 on all the derived values of k_0 and k_∞.

3.4. Temperature dependence of k_1 and k_2

Temperature dependences of the low and high pressure limits of k_1 and k_2 are shown in Fig. 10 and 11, respectively. One can note good agreement between the results obtained from the kinetics of the nitrate loss and those of the products formation. The combination of two approaches allowed the determination of the rate constants over a range of nearly 5 orders of magnitude.

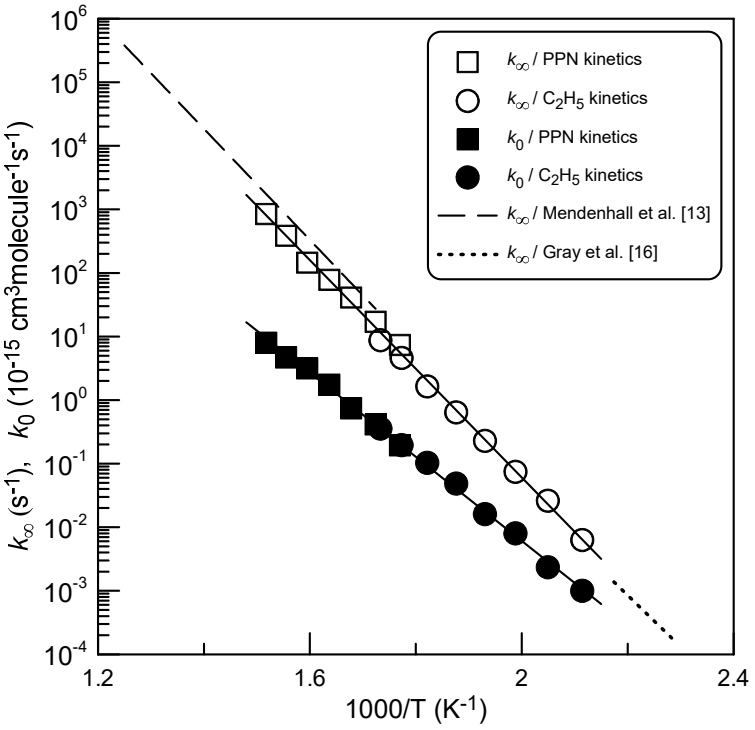

Fig. 10 Thermal decomposition of n-propyl nitrate: temperature dependence of the high and low pressure limits of k_1.

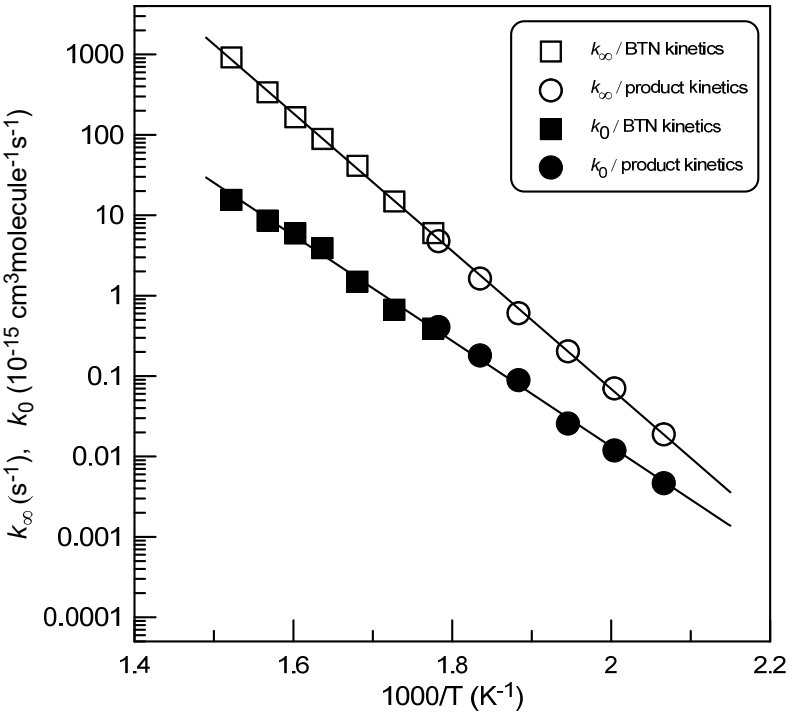

Fig. 11 Thermal decomposition of n-butyl nitrate: temperature dependence of the high and low pressure limits of k_2.

Unweighted exponential fit to the experimental data in Fig. 10 and 11 provides the following Arrhenius expressions: k_∞ (PPN) = 7.46× 10^{15} exp(-19675/T) s^{-1} and k_0 (PPN) = 1.02× 10^{-4} exp(-15225/T) $cm^3molecule^{-1}s^{-1}$, k_∞ (BTN) = 9.54× 10^{15} exp(-19732/T) s^{-1} and k_0 (BTN) = 1.78× 10^{-4} exp(-15115/T) $cm^3molecule^{-1}s^{-1}$.

In the above analysis, the temperature dependence of the low and high pressure limits of the rate constant was determined from the individual values of these parameters determined at each temperature. We applied also another approach which consisted of a global fitting of all the experimental data simultaneously accordingly to equations (I) and (II) with fixed and independent of temperature F_c = 0.6 and N = 1 and variable pre-exponential factors and activation energies in Arrhenius expressions for k_∞ and k_0. The expressions for k_∞ and k_0 obtained within this approach did not differ significantly from those presented above and are recommended from the present study:

k_∞ (PPN) = 7.34× 10^{15} exp(-19676/T) s^{-1},

394 k_0 (PPN) = 0.68× 10^{-4} exp(-15002/T) $cm^3 molecule^{-1} s^{-1}$,

395 k_∞ (BTN) = 7.49× 10^{15} exp(-19602/T) s^{-1}

396 k_0 (BTN) = 2.80× 10^{-4} exp(-15382/T) $cm^3 molecule^{-1} s^{-1}$

397 It should be emphasized again that the reported values of k_∞ and k_0 depend on the choice of
398 the F_c-value used in the fitting of falloff curves and should be considered just as parameters
399 allowing to represent the experimentally measured temperature and pressure dependence of k_1
400 and k_2 as:

401 $$k = \frac{k_0 k_\infty [M]}{k_0[M] + k_\infty} \times 0.6^{(1+(\log(\frac{k_0[M]}{k_\infty}))^2)^{-1}}$$

402 This expression in combination with k_∞ and k_0 given above reproduces all the
403 temperature and pressure dependence data obtained for k_1 and k_2 in the present study
404 with accuracy within 20 and 15%, respectively, and thus can be recommended for
405 calculation of k_1 and k_2 in the temperature ranges 473 – 659 K and 484 – 657 K,
406 respectively, and He pressures between 1 and 12.8 Torr with conservative uncertainty
407 of 20%.

408 As noted above the absolute values of k_∞ and k_0 determined in the present study depend
409 on the F_c-value used in the calculations. We conducted an analysis of the sensitivity of k_∞ and
410 k_0 to the choice of the F_c-value. For that the global fit of all the experimental data (shown in
411 Tables S1 and S2 of Supplementary data) to expressions (I) and (II) was performed using
412 different values of F_c. The results obtained for low and high pressure limits of k_1 and k_2 are
413 shown in Tables S3 and S4 (Supplementary data), respectively. The last columns in Tables S3
414 and S4 show the mean (for 75 and 65 experimental data points, respectively) of the ratios of
415 calculated (using expressions (I) and (II) with different F_c-factors and corresponding set of
416 Arrhenius parameters) and experimental values of k_1 and k_2, respectively. One can note that
417 the experimental rate constant data can be described adequately and with a similar precision

with any value of F_c between 0.3 and 0.8. On the other hand, the activation energies, E_∞ and E_0, are rather insensitive to the choice of F_c-factors, and seem to be well defined by the measured values of k_1 and k_2. Considering the data presented in Tables S3 and S4, we place less than 7% uncertainty on the activation energies in Arrhenius expressions for k_∞ and k_0 recommended above (for $F_c = 0.6$ and $N = 1$): E_∞ (PPN) = (19676 ± 600), E_0 (PPN) = (15002 ± 1000), E_∞ (BTN) = (19602 ± 500) and E_0 (BTN) = (15382 ± 500) K.

We failed to find in the literature any quantitative experimental data on thermal decomposition of n-butyl nitrate. Concerning n-propyl nitrate, to our knowledge, the quantitative data on its decomposition were reported only in two previous publications [13,16]. Mendenhall et al. [13], applying RRKM theory to the experimental data from their Very-Low-Pressure study of PPN pyrolysis at T = (580 – 800) K, derived the high pressure rate expression of k_1, k_∞ (PPN) = 3.16×10^{16} exp(-20118/T) s^{-1}. Gray et al. [16], referring to Ph.D thesis of L. Phillips (London, 1949), reported k_∞ (PPN) = 5.01×10^{14} exp(-18600/T) s^{-1} in rather narrow temperature range T = (438 – 460) K. The values of k_∞ (PPN) calculated with these expressions are shown in Fig. 10 and seem to be in satisfactory agreement with those from the present study.

The activation energies obtained in the present work for k_∞, E_∞ (PPN) = 39.1 ± 1.2 and E_∞ (BTN) = 38.9 ± 1.0 kcal mol^{-1}, allows the determination of the O–NO_2 bond dissociation energy (BDE) in n-propyl and n-butyl nitrates as BDE = $E_\infty - RT_{av}$, where T_{av} is the average temperature of the T-range used in experiments:

BDE (C_3H_7O-NO_2) = 38.0 ± 1.2 kcal mol^{-1}

BDE (C_4H_9O-NO_2) = 37.8 ± 1.0 kcal mol^{-1}

These values are in good agreement with the O–NO_2 bond dissociation energy of 38.3 and 38.2 kcal mol^{-1} in n-propyl and n-butyl nitrates, respectively, calculated by Khrapkovskii et al. [29] using density-functional B3LYP method. Zeng et al. [30]

using different DFT methods calculated O–NO_2 bond dissociation energy in n-propyl nitrate in the range (34.1-42.2) kcal mol^{-1}, which overlaps the experimental value from this work. It seems that the extensive experimental data from the present study could serve as a basis for further theoretical developments.

4. Conclusions

In this work, kinetics and products of the thermal decomposition of n-propyl and n-butyl nitrates were investigated. The rate constants of the reactions were measured as a function of temperature, T = (473-659) K, in the pressure range (0.95-12.8) Torr of helium. NO_2 was directly observed as a primary product of the decomposition of both nitrates and its yield (nearly unity) was measured. The co-product of NO_2 in the decomposition of n-propyl nitrate, propoxy radical C_3H_7O, was found to rapidly decompose on the timescale of our experiments leading to practically exclusive production of C_2H_5 radical and formaldehyde in the temperature range of the study. In contrast, for the butoxy radical ($CH_3(CH_2)_3O$), formed in a first stage of n-butyl nitrate decomposition, both decomposition to propyl radical and formaldehyde and isomerization to hydroxybutyl radical, $C^{\bullet}H_2(CH_2)_3OH$, was observed. The O-NO_2 bond dissociation energy in n-propyl and n-butyl nitrates were determined as (38.0 ± 1.2) and (37.8 ± 1.0) kcal mol^{-1}, respectively.

Acknowledgements

This work was supported by French National Research Agency (ANR) (ANR-12-BS06-0017-02). J. M. is very grateful for his PhD grant from CAPRYSSES project (ANR-11-LABX-006-01) funded by ANR through the PIA (Programme d'Investissement d'Avenir).

Appendix A. Supplementary data

Supplementary data associated with this article can be found, in the online version, at ...

References

[1] B.J. Finlayson-Pitts and J.N.J. Pitts, *Chemistry of the Upper and Lower Atmosphere: Theory, Experiments and Applications*, Academic Press, San Diego, 2000, p. 969.

[2] K.C. Clemitshaw, J. Williams, O.V. Rattigan, D.E. Shallcross, K.S. Law and R. Anthony Cox, *J. Photochem. Photobio. A*, 102, (1997) 117.

[3] P.Q.E. Clothier, B.D. Aguda, A. Moise and H.O. Pritchard, *Chem. Soc. Rev.*, 22, (1993) 101.

[4] T. Inomata, J.F. Griffiths and A.J. Pappin, *Symp. Int. Combust.*, 23, (1991) 1759.

[5] A. Toland and J.M. Simmie, *Combust. Flame*, 132, (2003) 556.

[6] H.J. Curran, *Int. J. Chem. Kinet.*, 38, (2006) 250.

[7] L. Phillips, *Nature*, 160, (1947) 753.

[8] G.K. Adams and C.E.H. Bawn, *Trans. Faraday Soc.*, 45, (1949) 494.

[9] J.B. Levy, *J. Am. Chem. Soc.*, 76, (1954) 3790.

[10] F.H. Pollard, H.S.B. Marshall and A.E. Pedler, *Trans. Faraday Soc.*, 52, (1956) 59.

[11] T.J. Houser and B.M.H. Lee, *J. Phys. Chem.*, 71, (1967) 3422.

[12] J.F. Griffiths, M.F. Gilligan and P. Gray, *Combust. Flame*, 24, (1975) 11.

[13] G.D. Mendenhall, D.M. Golden and S.W. Benson, *Int. J. Chem. Kinet.*, 7, (1975) 725.

[14] I.S. Zaslonko, V.N. Smirnov and A.M. Tereza, *Kinet. Catal.*, 34, (1993) 531.

[15] J.C. Oxley, J.L. Smith, E. Rogers, W. Ye, A.A. Aradi and T.J. Henly, *Energy Fuels*, 14, (2000) 1252.

[16] P. Gray, R. Shaw and J.C.J. Thynne, *Prog. React. Kinet.*, 4, (1967) 63.

[17] J. Morin and Y. Bedjanian, *J. Phys. Chem. A*, 120, (2016) 8037.

[18] J. Morin, M.N. Romanias and Y. Bedjanian, *Int. J. Chem. Kinet.*, 47, (2015) 629.

[19] R.S. Timonen, J.A. Seetula and D. Gutman, *J. Phys. Chem.*, 94, (1990) 3005.

[20] J. Morin, Y. Bedjanian and M.N. Romanias, *Int. J. Chem. Kinet.*, 48, (2016) 822.

[21] R. Boschan, R.T. Merrow and R.W. van Dolah, *Chem. Rev.*, 55, (1955) 485.

[22] J. Troe, *Chem. Rev.*, 103, (2003) 4565.

[23] J. Troe, *J. Phys. Chem.*, 83, (1979) 114.

[24] S.P.S. J. B. Burkholder, J. Abbatt, J. R. Barker, R. E. Huie, C. E. Kolb, M. J. Kurylo, V. L. Orkin, D. M. Wilmouth, P. H. Wine . in, JPL Publication 15-10, Jet Propulsion Laboratory, Pasadena, 2015 http://jpldataeval.jpl.nasa.gov.

[25] A. Rauk, R.J. Boyd, S.L. Boyd, D.J. Henry and L. Radom, *Can. J. Chem.*, 81, (2003) 431.

[26] P. Zhang, S.J. Klippenstein and C.K. Law, *J. Phys. Chem. A*, 117, (2013) 1890.
[27] S.G. Bayliss, R.L. Failes and J.S. Shapiro, *Can. J. Chem.*, 59, (1981) 1827.
[28] R. Atkinson, D.L. Baulch, R.A. Cox, J.N. Crowley, R.F. Hampson, R.G. Hynes, M.E. Jenkin, M.J. Rossi and J. Troe, *Atmos. Chem. Phys.*, 6, (2006) 3625.
[29] G.M. Khrapkovskii, T.F. Shamsutdinov, D.V. Chachkov and A.G. Shamov, *J. Mol. Struct.: THEOCHEM*, 686, (2004) 185.
[30] X.-L. Zeng, W.-H. Chen, J.-C. Liu and J.-L. Kan, *J. Mol. Struct. - THEOCHEM*, 810, (2007) 47.

Figure captions

Fig. 1 Diagram of the flow reactor.

Fig. 2 Example of kinetics of n-propyl nitrate decomposition at different pressures of He in the reactor: T = 627 K.

Fig. 3 Rate of n-propyl nitrate decomposition measured at different temperatures from kinetics of the nitrate loss as a function of total pressure of He. Uncertainty on k_1 (nearly 10%) corresponds to the size of symbols. Continuous lines represent the best fit to the experimental data according to equations (I) and (II) with $F_c = 0.6$ and two varied parameters, k_0 and k_∞.

Fig. 4 Rate of n-butyl nitrate decomposition measured at different temperatures from kinetics of BTN loss as a function of total pressure of He. Uncertainty on k_2 (nearly 10%) corresponds to the size of symbols. Continuous lines represent the best fit to the experimental data according to equations (I) and (II) with $F_c = 0.6$ and two varied parameters, k_0 and k_∞.

Fig. 5 Concentration of the products formed upon decomposition of n-propyl nitrate as a function of consumed concentration of PPN: P = 8.5 Torr, T = 630 K. Error bars correspond to 10% uncertainty on the measurements of the PPN and product concentrations.

Fig. 6 Concentration of the products formed upon decomposition of n-butyl nitrate as a function of consumed concentration of BTN: P = 4 Torr, T = 640 K. Error bars correspond to characteristic 10% uncertainty on the measurements of the concentrations of BTN and reaction products.

Fig. 7 Kinetics of C_2H_5 production upon PPN decomposition measured at different pressures in the reactor: T = 549 K, [PPN] = 3.0×10^{13} molecule cm^{-3}.

Fig. 8 Rate constant of C_2H_5 production upon PPN decomposition as a function of total pressure of He at different temperatures in the reactor. Height of the symbols corresponds to nearly 15% uncertainty on k_1.

Fig. 9 Rate constant of reaction (2) measured from the kinetics of 1-bromopropane and 4-bromo-1-butanol production upon BTN decomposition in the presence of Br_2 as a function of total pressure of He at different temperatures in the reactor. Height of the symbols corresponds to nearly 15% uncertainty on k_2.

Fig. 10 Thermal decomposition of n-propyl nitrate: temperature dependence of the high and low pressure limits of k_1.

Fig. 11 Thermal decomposition of n-butyl nitrate: temperature dependence of the high and low pressure limits of k_2.